Shape-Dependent Evolution of Au@Ag Core–Shell Nanocrystals by PVP-Assisted N,N-Dimethylformamide Reduction

ARTICLE *in* CRYSTAL GROWTH & DESIGN · JUNE 2008

Impact Factor: 4.89 · DOI: 10.1021/cg800162t

CRYSTAL GROWTH & DESIGN
2008
VOL. 8, NO. 7
2528–2536

Shape-Dependent Evolution of Au@Ag Core−Shell Nanocrystals by PVP-Assisted *N,N*-Dimethylformamide Reduction

Masaharu Tsuji,*[,†,‡] Ryoichi Matsuo,[‡] Peng Jiang,[†,§] Nobuhiro Miyamae,[‡] Daisuke Ueyama,[‡] Michiko Nishio,[‡] Sachie Hikino,[†] Hisayo Kumagae,[†] Khairul Sozana Nor Kamarudin,[†,||] and Xin-Ling Tang[‡]

Institute for Materials Chemistry and Engineering, Kyushu University, Kasuga 816-8580, Japan, Graduate School of Engineering Sciences, Kyushu University, Kasuga 816-8580, Japan, National Center for Nanoscience and Technology, Beijing 100080, People's Republic of China, and Department of Gas Engineering, Faculty of Chemical and Natural Resources Engineering, Universiti Teknologi Malaysia, 81310 UTM Skudai, Johor, Malaysia

Received February 12, 2008; Revised Manuscript Received March 17, 2008

ABSTRACT: Shape-dependent Au@Ag core−shell nanocrystals have been successfully synthesized by using a two-step method. First, Au nanocrystal seeds with various shapes including single-crystal octahedron, single-twinned triangle or hexagon plate, and multiple-twinned decahedron were prepared by reducing $HAuCl_4$ in ethylene glycol (EG) in the presence of polyvinylpyrrolidone (PVP) as a polymer surfactant under the condition of microwave heating. Subsequently, thus-obtained Au seeds were added into *N,N*-dimethylformamide (DMF) solution containing Ag^+ ions for overgrowth of Ag shells by an oil-bath heating. Transmission electron microscope (TEM) observation demonstrates that shapes of formed Ag shells strongly depend on shapes of initiated Au seeds. These newly produced triangular or hexagonal platelike, octahedral, and multiple-twinned decahedral Au@Ag nanocrystals are mainly dominated by the Ag shells having {111} facets. This case is completely different from that previously investigated by us in EG system where formed triangular-bipyramidal, cubic, and pentagonal rod/wire Au@Ag core−shell nanostructures are surrounded by the Ag shells with {100} facets. Our studies reveal that it is possible to controllably prepare the Au@Ag core/shell nanocrystal structures with optional uniform crystalline planes by the same Au seed source and different reaction solvent.

Introduction

In recent years, bimetallic nanoparticles have received intensive attention owing to their novel optical, electronic, magnetic, and catalytic properties different from individual metals. Since these properties strongly depend on composition, shape, and size of the nanoparticles, extensive studies have been focused on the controlled synthesis of the composition and morphology of bimetallic core−shell and alloy nanoparticles.[1–3] Noble metal gold (Au) and silver (Ag) have the same face-centered cubic (fcc) crystal structure. Their lattice constants (Au (0.408 nm), Ag (0.409 nm)) are very similar. Some studies have shown that Au and Ag can form various alloy and Au@Ag core−shell nanocrystal structures.[4–19] For the Au@Ag core−shell nanostructures, a direct approach to determining the structure is to see the core−shell structure by transmission electron microscopy (TEM), because a clear boundary between Au and Ag elements can be distinguished by bright and dark contrast in TEM imaging.[6,9] Therefore, it is possible to deduce the evolution process of the final obtained Au@Ag core−shell nanocrystal structures by analyzing their TEM images.

Recently, we have succeeded in preparing Au@Ag core−shell nanocrystals by using a microwave (MW)−polyol method.[20,21] When $HAuCl_4 \cdot 4H_2O$ was reduced in ethylene glycol (EG) in the presence of polyvinylpyrrolidone (PVP) as a polymer surfactant, a mixture of single-crystal octahedral, single-twinned triangular platelike, and multiple-twinned decahedral Au nanocrystals was obtained. Although these Au nanoparticles possess different shapes, a common feature is that they are mainly surrounded by {111}-type facets. Once Ag^+ ions were reduced by using these Au nanocrystals as seeds in EG solution, cubic, triangular-bipyramidal, and rod/wire Ag shells with {100}-type dominant facets were epitaxially formed around these seeds. We have concluded that morphology change between Au cores and Ag shells originates probably from the change in the adsorption selectivity of PVP molecules from Au {111}-type facets to Ag {100}-type ones in EG solvent.

We have also demonstrated an important role of chloride (Cl^-) anions in the formation process of Au@Ag core−shell nanocrystals in EG.[22] The effects of Cl^- ions on the Au@Ag nanocrystals have been investigated by systematically changing Cl^- concentration in Au seed solutions using NaCl as a precursor. We have found that few Au@Ag core−shell nanocrystals can be formed in the absence of Cl^- ions, while superfluous Cl^- ion concentration causes the formation of AgCl, which can interfere with evolution of the Au@Ag nanocrystals. A suitable small amount of Cl^- anions (0.3−3 mM) is necessary for the preparation of the Au@Ag nanocrystals. The growth mechanism of the Au@Ag nanocrystals can be reasonably explained in terms of shape selective crystal growth and oxidative etching of the Ag shells by Cl^-/O_2 (dissolved in solvent). Under our experimental conditions, spherical Ag particles are etched and gradually disappear, while the Ag shells with single crystal cubic, single-twinned bipyramidal, and five-twinned nanorod/-wire structures can survive and further grow into regular Au@Ag core−shell nanocrystal structures with clear facets and sharp edges. For the Au@Ag core−shell nanocrystals, favorable facets of the Ag shells grown epitaxially by Au seeds in EG are {100}-type planes. The Ag nanocrystals surrounded by {100} facets have been widely synthesized by a polyol method.[23–25]

Recently, Gao et al.[26] found that decahedral Ag nanocrystals having {111} facets could be prepared in high yields when

* To whom correspondence should be addressed. E-mail: tsuji@cm.kyushu-u.ac.jp.
† Institute for Materials Chemistry and Engineering, Kyushu University.
‡ Graduate School of Engineering Sciences, Kyushu University.
§ National Center for Nanoscience and Technology.
|| Universiti Teknologi Malaysia.

10.1021/cg800162t CCC: $40.75
Published on Web 06/06/2008

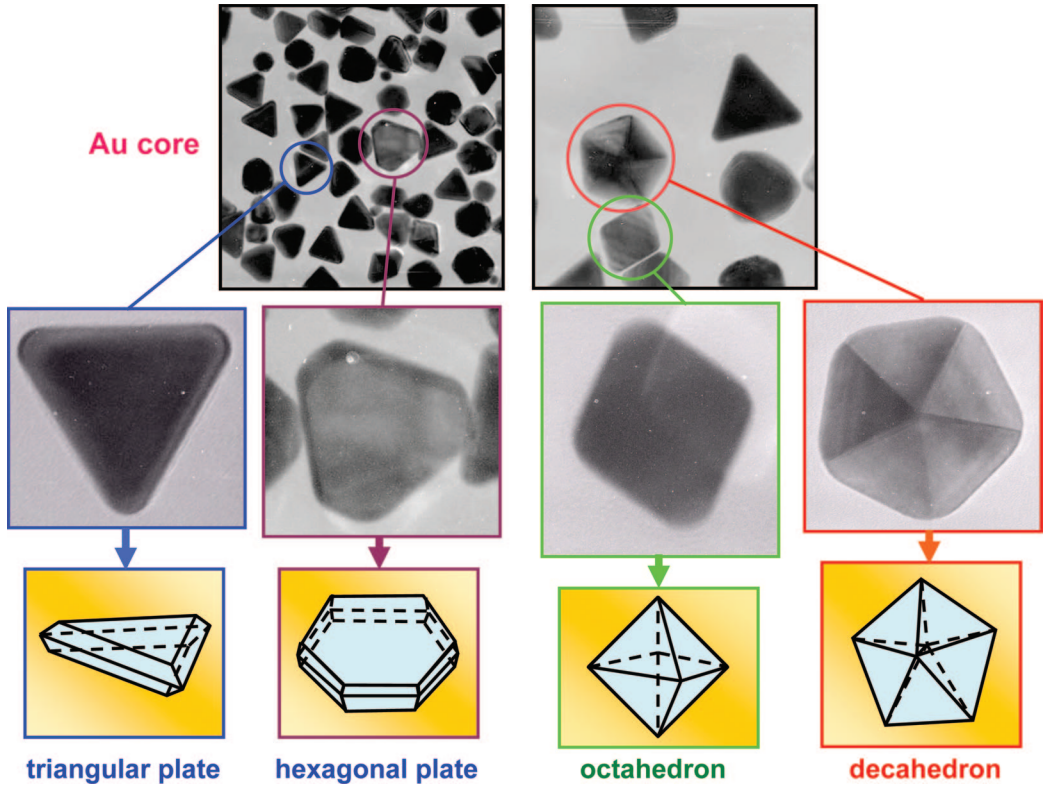

Figure 1. TEM images of the Au core nanocrystals prepared in the $HAuCl_4 \cdot 4H_2O$ (2.4 mM)/PVP (40 k, 1 M)/EG solution system by MW heating for 3 min.

reducing $AgNO_3$ in *N,N*-dimethylformamide (DMF) solution with an assistance of PVP (Mw = 1,300 k) under the condition of conventional oil-bath heating. Based on TEM and SEM observation of obtained products, they proposed that decahedral Ag nanocrystals are assembled from five tetrahedrons step by step. An important suggestion in their work is that favorable facets of Ag nanocrystals prepared in DMF solution can be changed from {100}-type in EG to {111}-type in DMF.

In this paper, we will report new Au@Ag core−shell nanocrystal structures synthesized in DMF solution containing Ag^+ ions by using various shaped Au nanoparticles as seeds. Au@Ag core−shell nanocrystals were prepared at different $[AgNO_3]/[HAuCl_4]$ molar ratios to examine their growth mechanisms. TEM images of the Au@Ag core−shell nanocrystal products provide new valuable information on possible evolution process of each kind of Au@Ag core−shell nanocrystal in DMF under the presence of PVP.

Experimental Section

In our experiments, EG and DMF were used as both reductant and solvent. The preparation of Au@Ag core−shell nanocrystals has been carried out by two separate steps. At first step, Au nanocrystal seeds were prepared by a MW heating in EG, which was similar to that reported previously.[20–22] In the process, 2.4 mM of $HAuCl_4 \cdot 4H_2O$ was resolved in 20 mL of EG solvent. Then, 1 M of PVP (Mw = 40 k in terms of monomeric units) was added into the above solution. The whole reaction system was heated for 3 min by a MW irradiation in a CW mode (Shikoku Keisoku, μ Reactor, 400 W). After naturally cooling down to room temperature, Au seeds were separated and obtained from EG/C_2H_5OH solution by centrifuging the colloidal solution at 15,000 rpm for 25 min. At the second step, Au seeds were added into DMF solution (30 mL) containing 126 mM of PVP (Mw = 1,300 k). Then, various amounts of $AgNO_3$ were added into corresponding Au seed solutions in terms of different $[AgNO_3]/[HAuCl_4]$ molar ratios from 1 to 18, respectively. These solutions were separately heated in an oil bath at 140 °C for 3 h. Product solutions were centrifuged at 13,000 rpm for 60 min. The precipitates were collected, and then redispersed in deionized water, respectively. For TEM (JEOL JEM-2010) observation, samples were prepared by dropping colloidal solutions of the products on carbon-coated Cu grids. Absorption spectra of the product solutions were measured in the UV−visible (vis)-near infrared (NIR) region using a Shimadzu UV-3600 spectrometer.

Results and Discussion

Crystal Structures of Au Seeds. Figure 1 shows typical TEM images of the Au nanocrystals obtained by reducing $HAuCl_4 \cdot 4H_2O$ in EG under the condition of MW heating for 3 min. A mixture of spherical, triangular, hexagonal, octahedral, and pentagonal Au nanoparticles is found. Morphologies and corresponding crystal structures of these Au nanocrystals, shown in Figure 1, have been positively evidenced by further inclined-angle TEM observation and selected area electron diffraction (SAED) experiments, as reported previously.[21,22] Fractions of spherical, triangular and hexagonal platelike, octahedral, and decahedral particles were 33, 21, 37, and 9%, respectively.

In general, different crystal planes exhibit different surface energies for fcc crystals. For low index planes, the surface energy order is $\gamma_{\{111\}} < \gamma_{\{100\}} < \gamma_{\{110\}}$.[27] According to Wulff's rule, the possibility for the fcc nanocrystals surrounded by {111} and/or {100} facets becomes large in final thermodynamic equilibrium shapes.[28] In principle, fcc crystals can possess various shapes covered by {111} and/or {100} facets due to possible dynamic routes during the process of crystal nucleation

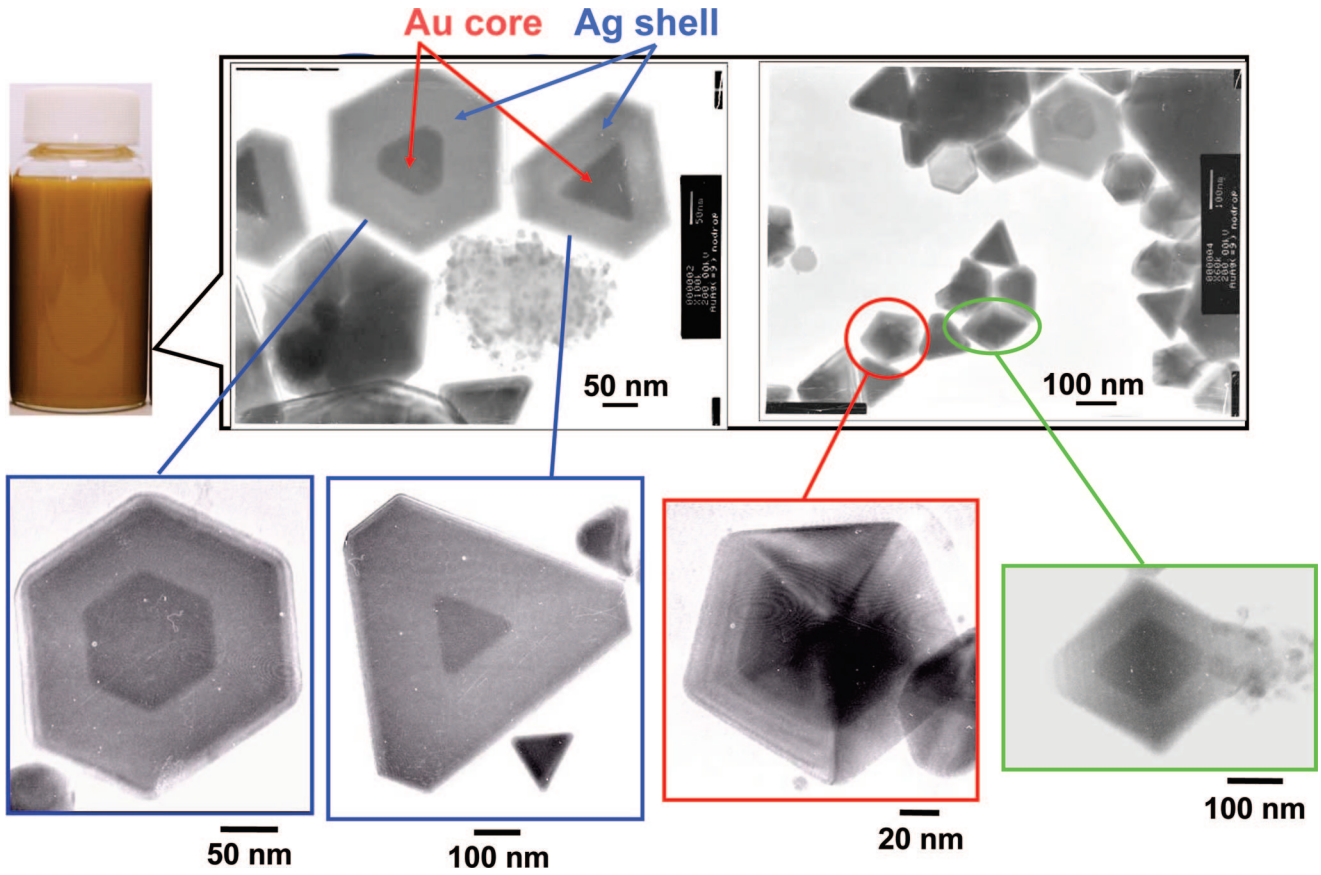

Figure 2. TEM images of the Au@Ag nanocrystals prepared in the Au seeds/$AgNO_3$ (21.6 mM)/PVP (1,300 k, 1 M)/DMF solution system by an oil-bath heating for 3 h.

and growth.[27] The crystal facets having faster growth rates disappear, and those having slower growth rates finally remain. The difference of growth rates along various crystal plane directions dominates possible shapes of obtained product. Under the condition of rapid MW heating, where crystal shapes are not determined by thermodynamic equilibrium shapes but dynamic ones, site-selective growth due to face-selective adsorption of surfactant occurs. It is worth noting that octahedral single-crystal Au nanocrystals, twinned triangular Au plates, and multitwinned decahedral (MTD) Au nanocrystals obtained in this study are surrounded solely by the most stable {111}-type facets, while twinned hexagonal Au plates also have six {100}-type side planes besides six {111}-type side planes and two top and bottom {111}-type planes.[27] This indicates that the formation of Au crystals with {111} facets is more favorable due to the selective adsorption of PVP to {111}-type facets of Au nanoparticles in EG under the condition of MW heating. An advantage of MW heating is that highly crystalline Au nanocrystals could be prepared in high yields due to local heating of nanoparticles by skin effect of MW.[29] In the oil-bath heating of the same reagent solution, it was difficult to prepare such highly crystalline Au nanocrystals and major products were spherical particles.[23a]

Au@Ag Core−Shell Nanocrystals Having {111} Facets. Figure 2 shows typical TEM images of products obtained after Au seeds are added into $AgNO_3$/DMF solution at an [$AgNO_3$]/[$HAuCl_4$] molar ratio of 9. From the TEM images, we can observe a mixture of Au@Ag core−shell nanocrystals with various shapes. Obviously, hexagonal and truncated-triangular platelike Ag shells are overgrown from triangular and hexagonal Au cores, respectively, whereas decahedral and octahedral Ag shells are overgrown from the decahedral and octahedral Au cores, respectively. In this condition, yields of platelike, octahedral, decahedral, and other nonpolygonal core−shell nanocrystals were 26, 10, 12, and 7%, respectively, which occupies 55% of total products. The rest of products were Ag nanocrystals.

In order to understand growth mechanisms of these Au@Ag core−shell particles, Au@Ag nanocrystals have been prepared at different [$AgNO_3$]/[$HAuCl_4$] molar ratios. Figures 3a−3d show TEM images of the Au cores and Au@Ag nanocrystals overgrown over triangular-plate, hexagonal-plate, octahedral, and decahedral Au cores at [$AgNO_3$]/[$HAuCl_4$] molar ratios of 1, 9, and 18, respectively. At low [$AgNO_3$]/[$HAuCl_4$] molar ratios of 1, thin triangular and hexagonal shells are epitaxially formed over the triangular and hexagonal Au plate cores (see Figures 3a and 3b). With the increase in the [$AgNO_3$]/[$HAuCl_4$] molar ratio, larger triangular, truncated-triangular, or hexagonal Ag shells are overgrown. The edge length of Ag shells enlarges with increase in the [$AgNO_3$]/[$HAuCl_4$] molar ratio. At the highest [$AgNO_3$]/[$HAuCl_4$] molar ratio of 18, Ag shell edges can achieve about 3 times longer than those of platelike Au cores, but Au cores are still observed easily at a constant contrast. This indicates that the Au@Ag core−shell particles have platelike shapes. In order to further confirm the crystal structures of triangular and hexagonal particles, TEM imaging has been carried out from different view angles within ±16° (Figure 4a). There is no significant change happening in bright and dark contrast of these triangular and hexagonal particles when inclining these Au@Ag core−shell nanocrystals in TEM observation. In contrast, we also demonstrate the TEM images of bipyramidal Au@Ag core−shell particle observed from different view angles, where significant bright and dark change

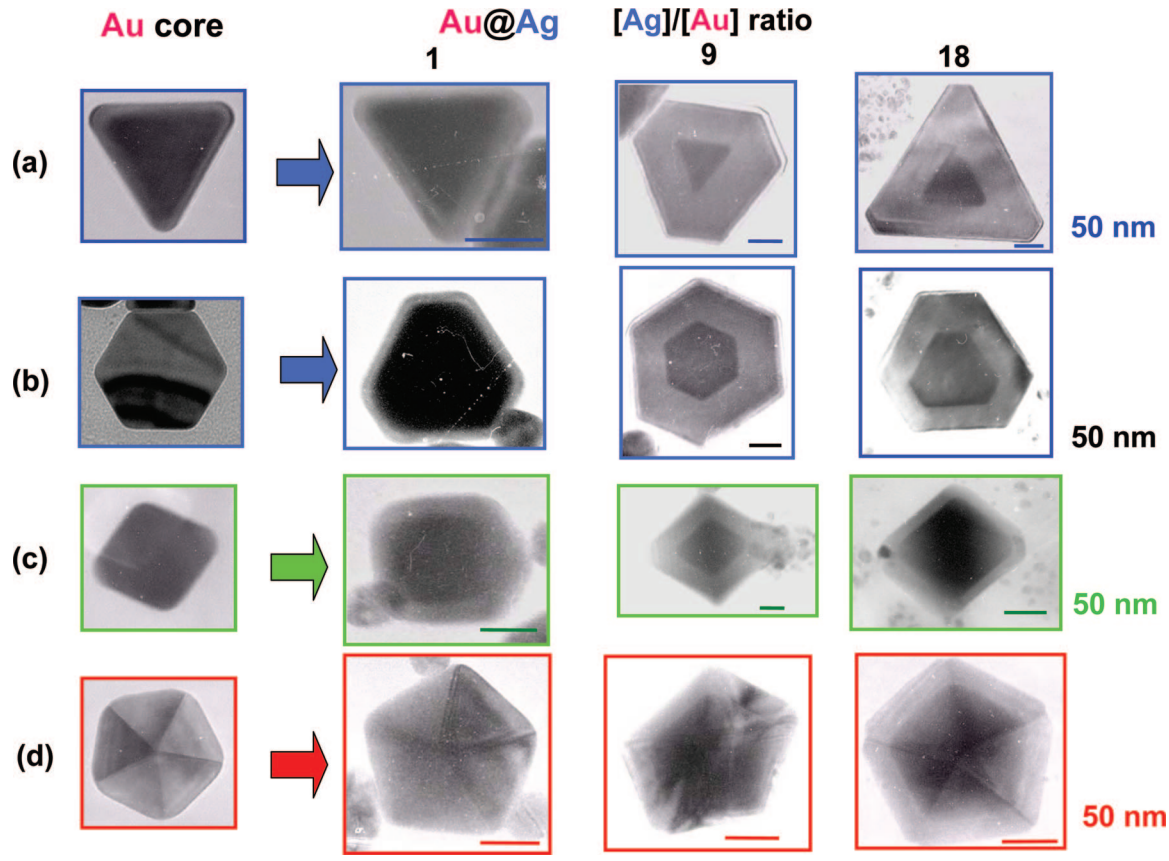

Figure 3. TEM images of the Au cores synthesized by a MW heating for 3 min and the Au@Ag nanocrystals prepared at different $[AgNO_3]/[H_2AuCl_4]$ molar ratios by an oil-bath heating.

can be observed (see Figure S1 in Supporting Information). The above findings led us to conclude that the triangular and hexagonal particles are indeed platelike, as shown in Figure 4b for the hexagonal plate. Extra evidence of the platelike structure can be provided by selected area electron diffraction (SAED) pattern (see Figure 4c) of the hexagonal particle, where, besides strong {220} reflections of fcc crystals, very weak forbidden 1/3{422} reflections are found. This implies the presence of a twinned plane within the {111} planes in the Au crystal plate along the perpendicular incident direction of the electron beam.[30]

Figures 3c and 3d show TEM photographs of Au core and Au@Ag nanocrystals overgrown on octahedral and decahedral Au cores at $[AgNO_3]/[HAuCl_4]$ molar ratios of 1, 9, and 18, respectively. It is clear that octahedral and decahedral Ag shells are overgrown into the same shapes as the Au cores. The sizes of octahedral and decahedral Ag shells also increase with the enhancement of the $[AgNO_3]/[HAuCl_4]$ molar ratio. At the highest $[AgNO_3]/[HAuCl_4]$ molar ratio of 18, their sizes can enlarge to about 1.5 times the original Au cores. This value is smaller than that of platelike Au@Ag nanocrystals.

Additional Growth Route of Decahedral Au@Ag Nanocrystals. Figure 5 shows a TEM image of Au@Ag nanocrystals obtained at a $[AgNO_3]/[HAuCl_4]$ molar ratio of 18. In this TEM image, decahedral Au@Ag nanocrystals evolved from different Au seed sources are observed, as marked by red and blue circles. The decahedral Ag shells labeled by red circles are overgrown from the decahedral Au cores, while those marked by blue circles only show that they seem to be grown from segments of decahedral Au cores. To shed light on the root of formation of the decahedral Au@Ag nanocrystals, more TEM images of the Au@Ag nanocrystals are analyzed. Figure 6a show TEM images of the Ag nanocrystals obtained from $AgNO_3$/PVP (1,300 k)/DMF solutions. These images clearly demonstrate that the decahedral Ag nanocrystals are grown step-by-step through tetrahedral component, as reported by Gao et al.[26] When carefully observing TEM images of the Au@Ag particles obtained at $[AgNO_3]/[HAuCl_4]$ molar ratios of 1, 9, and 18, we find bi-, tri-, and tetratetrahedral Ag shell nanocrystal structures, as shown in Figure 6b. SEM images of Au core nanocrystals also show the formation of thin bitriangular Au plates, corresponding to truncated bitetrahedral structure (see left image in Figure 6b). In addition, bi-, tri-, and tetratetrahedral Au@Ag nanocrystals containing thin Au bitriangular plates between two tetrahedrons are clearly observed. Therefore, for the decahedral Au@Ag nanocrystals, we think that two kinds of epitaxial growth processes probably occur. One kind is that decahedral Ag shells are epitaxially formed directly from decahedral Au seeds. Another kind is that truncated bitetrahedral Au seeds are first evolved into bitetrahedral Au@Ag core−shell nanocrystals and subsequently the Au@Ag nanocrystals grow into decahedral Au@Ag nanocrystals step by step, which is similar to the growth process suggested by Gao et al.[26]

Growth Mechanisms of Various Au@Ag Nanocrystals. The schematic crystal structures of various Au@Ag nanocrystals obtained in DMF using PVP (Mw = 1,300 k) by the two-step method are shown on right side in Figures 7a−7c. For comparison, those obtained in EG using PVP (Mw = 40 k) under the MW heating are shown on left side of the same figures. Twinned bitriangular Au core plates consist of two wide top and bottom {111} planes and six narrow {111} side facets. Ag shells with same shape can be epitaxially formed on the Au cores when the Au plates are very thin. Bihexagonal or bitruncated-triangular Au cores and Ag shells consist of two

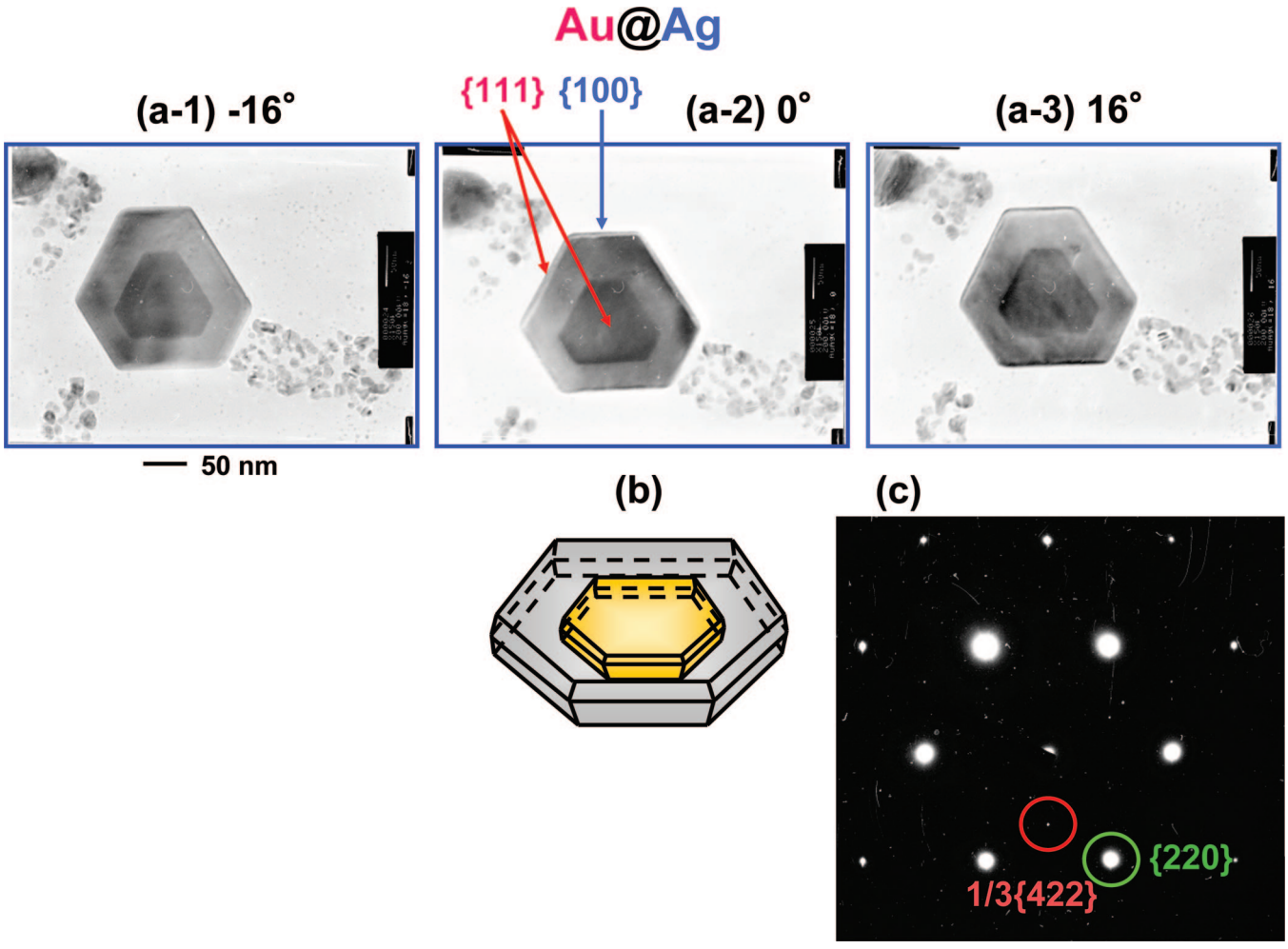

Figure 4. TEM images of hexagonal Au@Ag nanocrystal observed from different view angles and its crystal structure and SAED pattern.

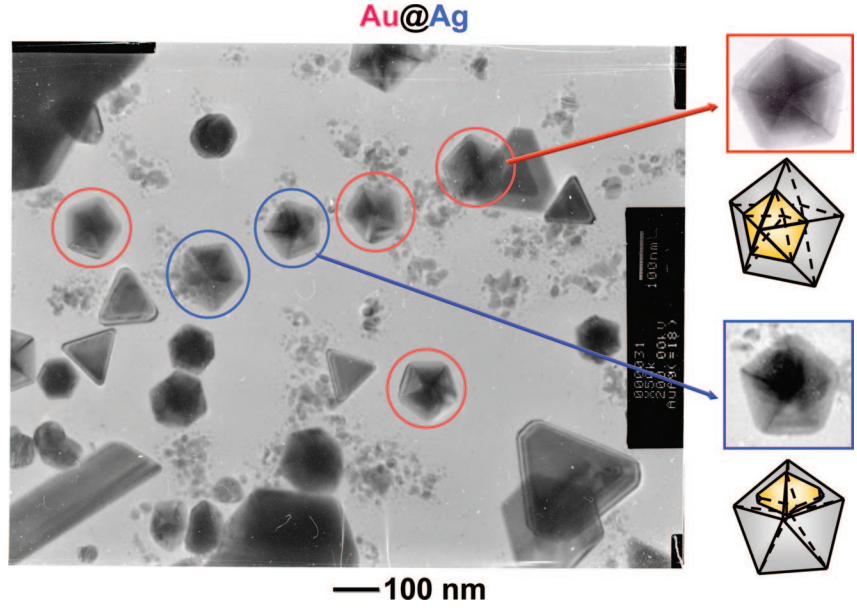

Figure 5. TEM images of two kinds of decahedral Au@Ag nanocrystals evolved from different Au core precursors in DMF and their crystal structures.

{111} top and bottom planes as well as six {111} and six alternative {100} side facets. Like bitriangular Au@Ag plates, bihexagonal Au@Ag core−shell plates can be epitaxially formed. Interestingly, we have observed that some bihexagonal Au plates are formed from bitriangular Au plate cores. In this case, whether side facets are {111} or {100} facets can be distinguished by observing direction of edge line of surfaces relative to that of the Au cores. Parallel edge lines of Au core

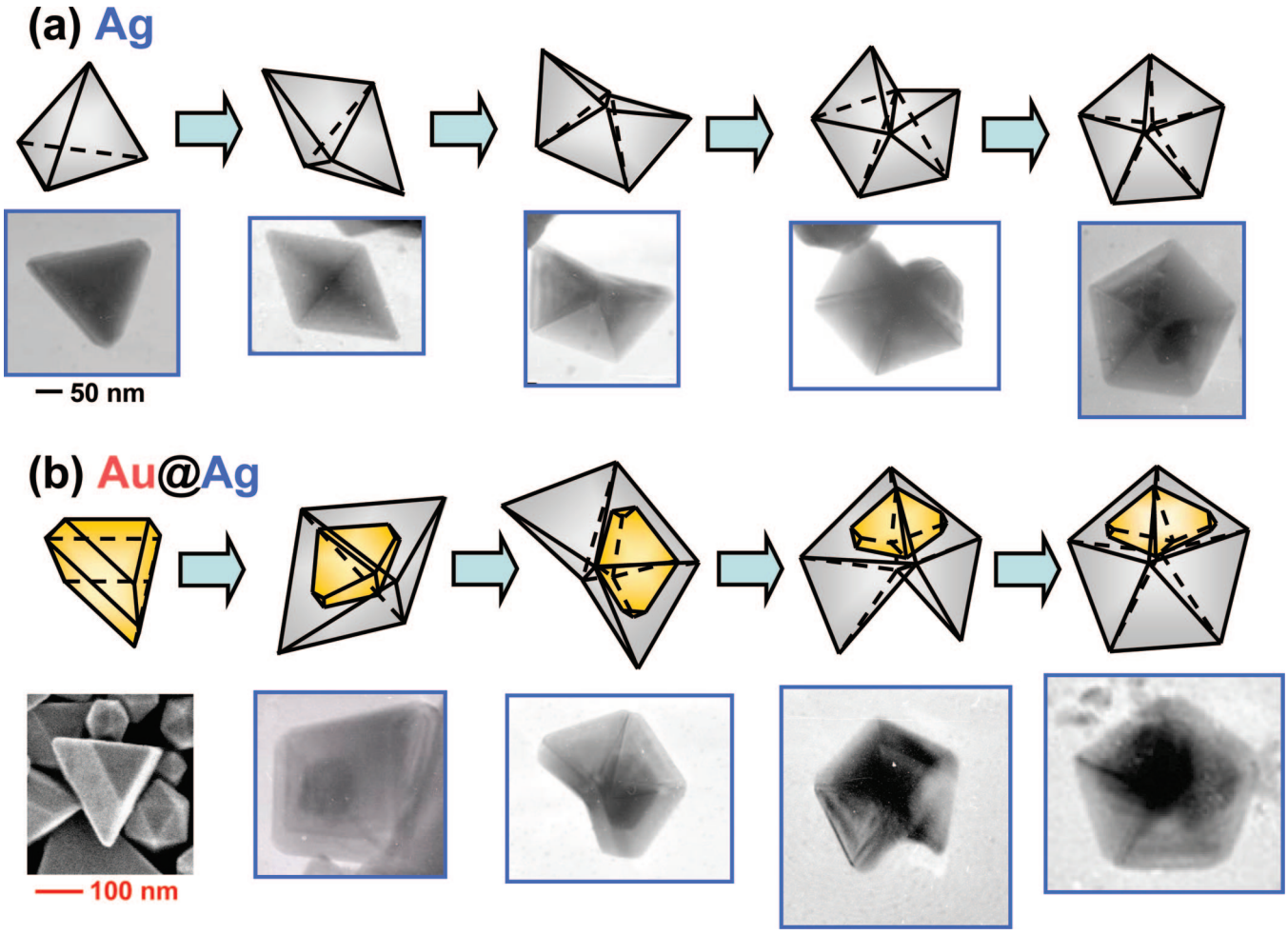

Figure 6. TEM images of decahedral Ag and Au@Ag nanocrystals prepared in DMF and their growth mechanisms.

and Ag shell show that side facets of Ag shells are {111}-type, because side facets of the Au cores are {111} facets. If they are not parallel, the side facets of the Ag shells are {100} type. Since no significant changes in TEM images have been observed in Figure 4a, only thin Ag shells are formed in the Au@Ag plates. This means that growth directions parallel to Au core plates are much faster than those along other directions because the twinning interface is more active. If the growth rates of the Ag shells along ⟨112⟩ directions are much faster than those along ⟨110⟩ directions, bitriangular Au@Ag core−shell plates are produced. Contrariwise, bihexagonal Au@Ag core−shell plates occur.

From thin triangular and hexagonal Au core plates, similar platelike Ag shells are overgrown. On the other hand, from a thick triangular Au core plate, the formation of bitetrahedrons is more favorable than that of thick platelike structures. This will be a main reason why pentagonal particles having thick bitriangular Au core plates are also formed. We found that all Ag shells are equally overgrown on the Au core, as shown in Figure 3d. However, we did not find the Au@Ag nanocrystals with decahedral Au cores and bi-, tri-, and tetratetrahedral Ag shells. It shows that growth of Ag shells on decahedral Au seeds does not obey a stepwise process.

Figures 7b and 7c schematically depict crystal structures of octahedral and decahedral Au@Ag core−shell nanocrystals. Octahedral and decahedral fcc crystals are composed of eight and ten stable {111} facets. Crystal growth of the Ag shells from octahedral and decahedral Au cores epitaxially occurs over these {111} facets. As a result, Au@Ag nanocrystals surrounded solely by {111} facets are produced. It should be addressed that the Ag shells deposited over Au cores in DMF have {111} facets, whereas those formed in EG have {100} facets. A detailed reason why such a dramatic change in shapes of the Ag shells between DMF and EG occurs is unclear now. One possible reason can be attributed to the difference in PVP adsorption selectivity on Ag nanostructures. PVP (Mw = 1,300 k) molecules prefer selectively to adsorb on the {111} facets of the Ag shells in DMF in comparison to favorable absorption of them (Mw = 40 k) on the {100} facets in EG. The selective adsorption of PVP molecules can affect the growth rate of adsorbed Ag facets. Finally, Au@Ag nanocrystals with different Ag shell shapes are formed. To evaluate solvent effect on morphology of the Ag shell, we prepared Au@Ag nanostructures by using PVP (Mw = 40 k) in DMF. The majority of obtained product is surrounded by {111} facets as in the case of PVP (Mw = 1,300 k). Obviously, size of PVP molecule is not a main factor to determine final morphology of the formed Ag shell in the same reaction solvent. Therefore, another possible factor is solvent effect. It is the difference between DMF and EG solvents that induces the change in Ag shell shapes. Different reducing ability of Ag^+ between DMF and EG may also affect the change in Ag shell shapes.

Two points should be addressed for us in the formation of Au@Ag core−shell nanocrystals in DMF. One point is the shapes of the Ag nanocrystals prepared from the $AgNO_3$/PVP(1,300 k)/DMF solution without the presence of Au seeds.

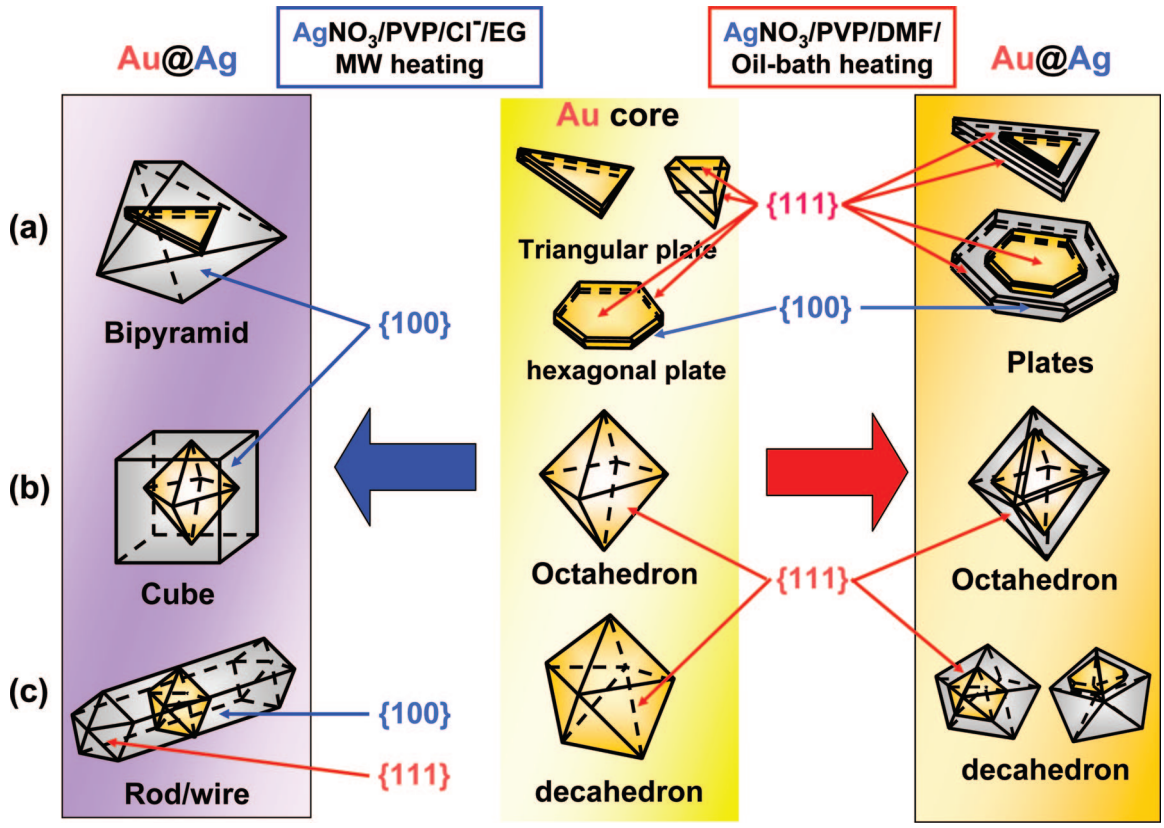

Figure 7. Schematic crystal structures of the Au cores and Au@Ag nanocrystals prepared in DMF by an oil-bath heating (right side) and in EG by a MW heating (left side).

They are triangle, truncated-triangle, hexagon, and decahedron. Some segments of decahedral Ag nanoparticles such as twinned bi-, tri-, and tetratetrahedrons also coexist in final products. Few octahedral Ag particles with single crystal structure occur. This shows that the Ag nanoparticles with twinned crystal structures are preferentially formed in DMF solution with the assistance of PVP (Mw = 1,300 k) molecules. If using Au seeds with octahedral shape, octahedral Ag shell can be easily epitaxially grown on the Au cores, leading to formation of the Au@Ag core−shell nanocrystal with octahedral shape. Since it is generally difficult to prepare octahedral Ag particles with {111} facets, the present technique is a new promising method for the synthesis of Ag nanocrystals with octahedral shape.

The second point is the preparation method of Ag shells. In present study, we can prepare Ag shells with {111} facets without the presence of Cl^- anions under the condition of oil-bath heating. In our previous reports on the Ag nanostructures with well-defined {100} facets by MW heating, a small amount of Cl^- anion was necessary.[23d] The role of Cl^- anions is oxidative etching of spherical particles, which is more favorable to the formation of single crystal cubes, single-twinned bipyramidal crystals, and five-twinned rods/wires having {100} facets. We have also prepared Ag shells under the condition of a MW heating in DMF as well as by a dropwise-injection method of $AgNO_3$ under the condition of oil-bath heating, which was widely used for preparation of Ag cubes and five-twinned rods/wires in EG.[24] For both cases, only small amounts of similar Au@Ag core−shell particles can be obtained. We have found that the optimal route for the preparation of the Ag shells with {111} facets is an oil-bath heating method at 140 °C for 3 h in one pot. In this case, all $AgNO_3$ and PVP were added to Au core solutions before oil-bath heating. In general, growth of highly crystalline nanocrystals usually requires slow reaction rate and longer reaction time to reduce the number of nucleation sites formed or equilibrium dissolution of these nucleation sites to promote site-specific growth. Such a site-selective slow crystal evolution can be probably established in the oil-bath heating process without the presence of Cl^-. Therefore, the Ag shells with well-defined {111} facets are formed over corresponding Au cores.

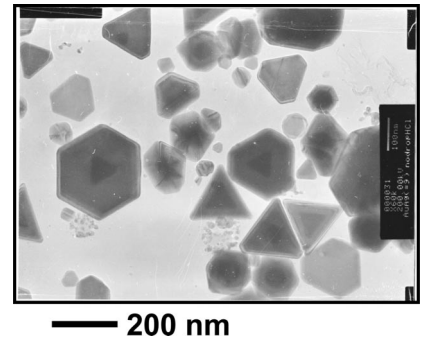

Figure 8. TEM image of the Au@Ag nanocrystals prepared in the Au seeds/$AgNO_3$ (21.6 mM)/HCl (0.3 mM)/PVP (1,300 k, 1 M)/DMF solution system by an oil-bath heating for 3 h.

We have also studied the effect of Cl^- anions on the formation of Au@Ag nanocrystals in DMF. Since NaCl is unresolved in DMF, HCl has been used as a precursor of Cl^- ion source. It has been found that Au@Ag nanocrystals having well-defined {111} facets and sharp edges can be produced by the addition of a small amount of Cl^- ions (0.3 mM) at second step (Figure 8). It shows that oxidative etching of Cl^-/O_2 (dissolved in DMF) is also useful for the further formation of Au@Ag nanocrystals with well-defined {111} facets at high yields.

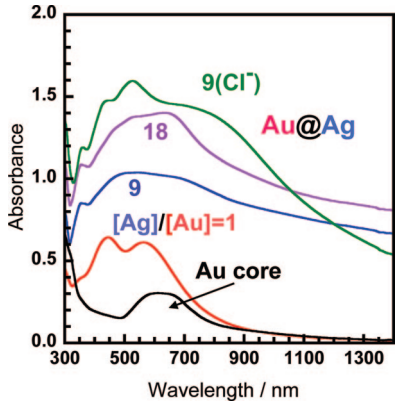

Figure 9. UV−vis−NIR absorption spectra of the Au core solution and Au@Ag core−shell nanocrystals obtained at various [$AgNO_3$]/[$HAuCl_4$] molar ratios and by the addition of HCl (0.3 mM) to the solution at a [$AgNO_3$]/[$HAuCl_4$] molar ratio of 9. Product solutions were diluted in EG by a factor of 25 before measurements.

UV−Vis−NIR spectra. Au@Ag nanocrystals in DMF gave brown solutions as shown Figure 2. Figure 9 shows UV−vis-NIR absorption spectra obtained at the [$AgNO_3$]/[$HAuCl_4$] molar ratios of 0, 1, 9, and 18. The absorption spectrum of Au core solution exhibits a broad surface plasmon resonance (SPR) peak in the 500−900 nm region with a peak at ∼600 nm. The spectrum of Au@Ag (molar ratio = 1) gives a more broad band in the 320−900 nm region with obvious double peaks at 450 and 560 nm. Although observed SPR bands of Ag nanoparticles depend on their size and shape, they are generally observed in the wavelength range of 320−800 nm with a peak at ∼420 nm.[23–25] The weak peaks of Au@Ag (molar ratio = 1) at ∼450 nm and ∼560 nm may be attributed to the SPR band of Ag shells and Au cores, respectively. In addition, the absorbance of the SPR band of Au@Ag increases with enhancement of the molar ratio of [$AgNO_3$]/[H_2AuCl_4] from 1 to 18. The SPR band becomes broader and broader with a long tail band. Similar broad spectral features are observed in the Au@Ag nanocrystals prepared in EG.[21] For comparison, the absorption spectrum obtained by the addition of a small amount of Cl^- is also shown. It should be noted that the SPR band becomes stronger by a factor of 60% than that in the absence of Cl^- in the peak position. Several obvious peaks can be observed clearly. This finding is consistent with the observation that the yield of Au@Ag nanocrystals with well-defined shapes and sharp edges increases by the addition of Cl^- anions.

Conclusion

Au@Ag core−shell nanocrystals have been prepared by using a two-step method. At the first step, a mixture of twinned triangular or hexagonal platelike, and multiple-twinned decahedral as well as single crystal octahedral Au nanocrystals all with {111} facets as dominant planes was prepared by a MW−polyol method in EG in the presence of PVP (Mw = 40 k). At the second step, when Ag^+ was reduced by using these Au nanocrystals as seeds in PVP (Mw = 1,300 k)/DMF in an oil-bath heating, Au@Ag core−shell nanocrystals were formed. They consist of triangular or hexagonal platelike, octahedral, and multiple-twinned decahedral Au@Ag nanocrystals surrounded by the Ag shells with {111} facets as main planes. These shapes of the Ag shells are different from those of Au@Ag nanocrystals prepared in EG by MW heating in the presence of a small amount of Cl^- ions where triangular-bipyramidal, cubic, and pentagonal rods/wires Ag nanostructures covered by the Ag shells with {100} facets are formed. These findings demonstrate that favorable facets and shapes of Ag shells can be effectively controlled by selecting different reaction solvents such as DMF and EG. Furthermore, addition of a small amount of Cl^- ions has been found to be effective for the preparation of Au@Ag nanocrystals with well-defined facets and sharp edges. Shape selective etching of unstable spherical particles in the nucleation and growth process will be similarly useful in the formation of highly crystalline Au@Ag nanoparticles under the present experimental conditions. In order to clarify why such dramatic changes occur by changing solvent and molecular weight of PVP, more investigations are needed.

Acknowledgment. We thank Mr. Naoki Ishigami for his measurements of SEM images. This work was supported by JST-CREST, Joint Project of Chemical Synthesis Core Research Institutions, and Grant-in-Aid for Scientific Research on Priority Areas "unequilibrium electromagnetic heating" and Grant-in-Aid for Scientific Research (B) from the Ministry of Education, Culture, Sports, Science, and Technology of Japan (Nos. 19033003 and 19310064).

Supporting Information Available: TEM images of triangular-bipyramidal Au@Ag nanocrystal observed from different view angles. This material is available free of charge via the Internet at http://pubs.acs.org.

References

(1) Toshima, N.; Yonezawa, T. *New J. Chem.* **1998**, *22*, 1179.
(2) Thomas, J. M.; Johnson, B. F. G.; Raja, R.; Sankar, G.; Midgley, P. A. *Acc. Chem. Res.* **2003**, *36*, 20.
(3) Scott, R. W. J.; Wilson, O. M.; Crooks, R. M. *J. Phys. Chem. B* **2005**, *109*, 692.
(4) Freeman, R. G.; Hommer, M. B.; Grabar, K. C.; Jackson, M. A.; Natan, M. J. *J. Phys. Chem.* **1996**, *100*, 718.
(5) Link, S.; Wang, Z. L.; El-Sayed, M. A. *J. Phys. Chem. B* **1999**, *103*, 3529.
(6) Hodak, J. H.; Henglein, A.; Giersig, M.; Harland, G. V. *J. Phys. Chem. B* **2000**, *104*, 11708.
(7) Mallik, K.; Mandal, M.; Pradhan, N.; Pal, T. *Nano Lett.* **2001**, *1*, 319.
(8) Mallin, M. P.; Murphy, C. J. *Nano Lett.* **2002**, *2*, 1235.
(9) Sibata, T.; Bunker, B. A.; Zhang, Z. Y.; Meisel, D.; Vardeman, C. F., II; Gezelter, J. D. *J. Am. Chem. Soc.* **2002**, *124*, 11989.
(10) Chen, D. H.; Chen, C. J. *J. Mater. Chem.* **2002**, *12*, 1557.
(11) Liu, M.; Guyot-Sionnest, P. *J. Phys. Chem. B* **2004**, *108*, 5882.
(12) Shankar, S. S.; Rai, A.; Ahmad, A.; Sastry, M. *J. Colloid Interface Sci.* **2004**, *275*, 496.
(13) Huang, C. C.; Yang, Z.; Chang, H. T. *Langmuir* **2004**, *20*, 608.
(14) Song, J. H.; Kim, F.; Kim, D.; Yang, P. *Chem. Eur. J.* **2005**, *11*, 910.
(15) Liu, F. K.; Huang, P. W.; Chang, Y. C.; Ko, F. H.; Chu, T. C. *Langmuir* **2005**, *21*, 2519.
(16) Xu, S.; Zhao, B.; Xu, W.; Fan, Y. *Colloids Surf. A: Physicochem. Eng. Aspects* **2005**, *257*, 313.
(17) Wilson, O. M.; Scott, R. W.; Garcia-Martinez, J. C.; Crooks, R. M. *J. Am. Chem. Soc.* **2005**, *127*, 1015.
(18) Pedersen, D. B.; Wang, S.; Duncan, E. J. S.; Liang, S. H. *J. Phys. Chem. C* **2007**, *111*, 13665.
(19) Rai, A.; Chaudhary, M.; Ahmad, A.; Bhargava, S.; Sastry, M. *Mater. Res. Bull.* **2007**, *42*, 1212.
(20) Tsuji, M.; Miyamae, N.; Matsumoto, K.; Hikino, S.; Tsuji, T. *Chem. Lett.* **2005**, *34*, 1518.
(21) Tsuji, M.; Miyamae, N.; Lim, S.; Kimura, K.; Zhang, X.; Hikino, S.; Nishio, M. *Cryst. Growth Des.* **2006**, *6*, 1801.
(22) Tsuji, M.; Nishio, M.; Jiang, P.; Miyamae, N.; Lim, S.; Matsumoto, K.; Ueyama, D.; Tang, X. *Colloids Surf., A* **2008**, *317*, 247.
(23) (a) Tsuji, M.; Hashimoto, M.; Nishizawa, Y.; Kubokawa, M.; Tsuji, T. *Chem. Eur. J.* **2005**, 11440. (b) Tsuji, M.; Nishizawa, Y.; Matsumoto, K.; Miyamae, N.; Tsuji, T.; Zhang, X. *Colloids Surf., A* **2007**, *293*, 185. (c) Tsuji, M.; Matsumoto, K.; Miyamae, N.; Tsuji, T.; Zhang, X. *Cryst. Growth Des.* **2007**, *7*, 311. (d) Tsuji, M.; Matsumoto, M.; Tsuji; Jiang, P.; Matsuo, R.; Tang, X.-L.; Kamarudin, K. S. N. *Colloids Surf., A* **2008**, *316*, 266.

(24) (a) Sun, Y.; Gates, B. Mayers.; Xia, Y. *Nano Lett.* **2002**, *2*, 165. (b) Sun, Y.; Yin, Y.; Mayers, B. T.; Herricks, T.; Xia, Y. *Chem. Mater.* **2002**, *14*, 4736. (c) Sun, Y.; Mayers, B.; Herricks, T.; Xia, Y. *Nano Lett.* **2003**, *3*, 955. (d) Wiley, B.; Sun, Y.; Mayers, B.; Xia, Y. *Chem. Eur. J.* **2005**, *11*, 454. (e) Chen, J.; Wiley, B. J.; Xia, Y. *Langmuir* **2007**, *23*, 4120. (f) Wiley, B. Y.; Sun, Y.; Xia, Y. *Acc. Chem. Res.* **2007**, *40*, 1067.

(25) (a) Gao, Y.; Jiang, P.; Liu, D. F.; Yuan, H. J.; Yan, X. Q.; Zhou, Z. P.; Wang, J. X.; Song, L.; Liu, L. F.; Zhou, W. Y.; et al. *Chem. Phys. Lett.* **2003**, *380*, 146. (b) Gao, Y.; Jiang, P.; Liu, D. F.; Yuan, H. J.; Yan, X. Q.; Zhou, Z. P.; Wang, J. X.; Song, L.; Liu, L. F.; Zhou, W. Y.; et al. *J. Phys. Chem. B* **2004**, *108*, 1287. (c) Gao, Y.; Jiang, P.; Song, L.; Liu, L.; Yan, X.; Zhou, Z.; Liu, D.; Wang, J.; Yuan, H.; Zhang, Z.; et al. *J. Phys. D: Appl. Phys.* **2005**, *38*, 1061. (d) Gao, Y.; Song, L.; Jiang, P.; Liu, L. F.; Yan, X. Q.; Zhou, Z. P.; Liu, D. F.; Wang, J. X.; Yuan, H. J.; Zhang, Z. X.; et al. *J. Cryst. Growth* **2005**, *276*, 606.

(26) Gao, Y.; Jiang, P.; Song, L.; Wang, J. X.; Liu, L. F.; Liu, D. F.; Xiang, Y. J.; Zhang, Z. X.; Zhao, X. W.; Dou, X. Y.; et al. *J. Cryst. Growth* **2006**, *289*, 376.

(27) Wang, Z. L. *J. Phys. Chem. B* **2000**, *104*, 1153.

(28) Tiller, W. A. *The science of crystallization: microscopic interfacial phenomena*; Cambridge University Press: Cambridge, 1991.

(29) (a) Tsuji, M.; Miyamae, N.; Hashimoto, M.; Nishio, M.; Hikino, S.; Ishigami, N.; Tanaka, I. *Colloids Surf., A* **2007**, *302*, 587. (b) Tsuji, M.; Miyamae, N.; Nishio, M.; Hikino, S.; Ishigami, N. *Bull. Chem. Soc. Jpn.* **2007**, *80*, 2024.

(30) Kirkland, A. I.; Jefferson, D. A.; Duff, D. G.; Edwards, P. P.; Gameson, I.; Johnson, B. F. G.; Smith, D. J. *Proc. R. Soc. London, A* **1993**, *440*, 589.

CG800162T